第 36 卷第 1 期 无 机 化 学 学 报 Vol.36 No.1
2020 年 1 月 CHINESE JOURNAL OF INORGANIC CHEMISTRY 165-172

两个三维柱层式单一手性配位化合物:合成、结构和性质

徐中轩* 柏雪累 蒙 琴
(遵义师范学院化学化工学院,遵义 563002)

摘要:在溶剂热合成条件下得到 2 个单一手性配位聚合物,即[Cd_3((*R*)-CIA)$_2$(bipy)$_{2.5}$(H_2O)$_2$]·*x*Guest (**1**)和[Zn_3((*R*)-CIA)(bmib)$_2$(H_2O)$_2$Cl]·H_2O·*x*Guest (**2**)((*R*)-H_3CIA =(*R*)-5-(1-羧基乙氧基)间苯二甲酸,bipy=4,4′-联吡啶,bmib=1,4-双(2-甲基-1*H*-咪唑-1-基)苯)。X 射线单晶结构分析揭示配合物 **1** 和 **2** 都是柱层式结构的三维框架。从拓扑分析的角度看,配位物 **1** 具有(3,3,3,6,6)-连接的网络,拓扑符号为$(4.5^2)_2(4.8^2)_2(4^2.6^8.8^3.10^2)(4^2.6^8.8^3.9^2)(5.8.9)_2$,而配合物 **2** 是(3,4,4)-连接的网络,拓扑符号为$(6\cdot7^2)_2(6\cdot7^5)_2(6^2\cdot7^4)$。此外,对上述配合物的热稳定性、圆二色谱和荧光性质也做了研究。

关键词:单一手性;乳酸衍生物;柱层式框架;拓扑
中图分号:O614.24$^+$2;O614.24$^+$1 **文献标识码**:A **文章编号**:1001-4861(2020)01-0165-08
DOI:10.11862/CJIC.2020.029

Two 3D Pillar-Layered Homochiral Coordination Complexes: Syntheses, Structures and Properties

XU Zhong-Xuan* BAI Xue-Lei MENG Qin
(*School of Chemistry and Chemical Engineering, Zunyi Normal College, Zunyi, Guizhou* 563002, *China*)

Abstract: Two homochiral coordination polymers [Cd_3((*R*)-CIA)$_2$(bipy)$_{2.5}$(H_2O)$_2$]·*x*Guest (**1**) and [Zn_3((*R*)-CIA)(bmib)$_2$(H_2O)$_2$Cl]·H_2O·*x*Guest (**2**) ((*R*)-H_3CIA=(*R*)-5-(1-carboxyethoxy) isophthalic acid, bipy=4,4′-bipyridine, bmib=1,4-bis(2-methyl-1*H*-imidazol-1-yl)benzene) were obtained under solvothermal reaction conditions. X-ray single crystal structure analysis reveals that complexes **1** and **2** are all 3D pillar-layered frameworks. From the viewpoint of structural topology, complex **1** possesses a (3,3,3,6,6)-connected net with a point symbol of $(4.5^2)_2(4.8^2)_2(4^2.6^8.8^3.10^2)(4^2.6^8.8^3.9^2)(5.8.9)_2$, while complex **2** is a (3,4,4)-connected net with a point symbol of $(6\cdot7^2)_2$ $(6\cdot7^5)_2$ $(6^2\cdot7^4)$. Moreover, thermal stabilities, CD spectra and luminescent properties of these new complexes have been studied. CCDC: 1920451, **1**; 1920452, **2**.

Keywords: homochiral; lactic acid derivative; pillar-layered framework; topology

Chirality as a basic feature of nature plays an important role in living system and artificial materials[1-2]. Current research on homochiral coordination polymers (HCPs) is rapidly expanding not only due to their intriguing architectures but also for their potential applications in enantioselective separation, chiral catalysis and so on[3-5]. Some synthetic strategies, including spontaneous resolution, asymmetric induction and use of chiral ligands, have been developed to construct HCPs[6-8]. Among them, the most effective method to build HCPs is to select an enantiopure compound as ligand to assemble with metal ions. Therefore, choice of chiral ligands is a key factor to obtain HCPs[9-10].

收稿日期:2019-06-05。收修改稿日期:2019-11-09。
国家自然科学基金(No.21761036)和贵州省科学技术基金(No.20181182)资助项目。
*通信联系人。E-mail:xuzhongxuan4201@163.com

As a semirigid chiral ligand, (*R*)-5-(1-carboxyethoxy)isophthalic acid ((*R*)-H_3CIA) (Scheme 1) was successfully synthesized from natural lactic acid and dimethyl 5-hydroxyisophthalate (Scheme 1a)[11]. Containing chiral lactate unit and rigid isophthalic acid unit, the (*R*)-H_3CIA has the following two advantages: (a) rigid carboxylate groups of isophthalic acid unit can efficiently construct interesting various structures; (b) the enantiopure lactate unit supplies the chiral source for construction of HCPs. Until now, (*R*)-H_3CIA has been used in the fabrication of related HCPs[12]. Moreover, to enhance the structural dimension and stability of HCPs, using nitrogenous compounds as auxiliary linkers is also a feasible method[13].

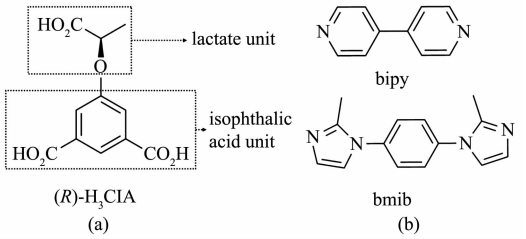

Scheme 1 Structures of the lactate derivative linker (a) and auxiliary N-donor ligands (b)

In order to further obtain characteristic HCPs of lactic acid, auxiliary bipy and bmib ligands were selected to assist (*R*)-H_3CIA to build HCPs (Scheme 1). Herein, two 3D HCPs, namely, $[Cd_3((R)\text{-}CIA)_2(bipy)_{2.5}(H_2O)_2]\cdot x$Guest (**1**) and $[Zn_3((R)\text{-}CIA)(bmib)_2(H_2O)_2Cl]\cdot H_2O\cdot x$Guest (**2**) (bipy=4,4′-bipyridine, bmib=1,4-bis(2-methyl-1*H*-imidazol-1-yl)benzene), were successfully synthesized under solvothermal conditions. In this work, we report their syntheses, crystal structures, thermal stabilities, CD spectra and luminescent properties.

1 Experimental

1.1 Materials and methods

All chemical reagents and solvents were commercially purchased and used without further purification except for (*R*)-H_3CIA, which was synthesized according to the documented procedures[11]. Elemental analysis was performed on a Perkin-Elmer 240C elemental analyzer. IR spectra were recorded as KBr pellets on a FTIR-650 FT-IR spectrometer from 400 to 4 000 cm^{-1}. The powder X-ray diffraction (PXRD) analysis was performed on a Rigaku Dmax2500 diffractometer (Voltage: 40 kV, Current: 40 mA) with Cu $K\alpha$ radiation (λ=0.154 056 nm) in a range of 5.00°~50.00°. Solid-state photoluminescence spectra were performed on a Hitachi FL-4500 fluorescence spectrophotometer. Solid CD spectra were measured on a MOS-450 spectropolarimeter.

1.2 Synthesis of $[Cd_3((R)\text{-}CIA)_2(bipy)_{2.5}(H_2O)_2]\cdot x$Guest (1)

A mixture of $Cd(NO_3)_2\cdot 4H_2O$ (62 mg, 0.2 mmol), bipy (31 mg, 0.2 mmol), (*R*)-H_3CIA (25 mg, 0.1 mmol) and pyrazine (80 mg, 1 mmol) was dissolved in 5 mL *N*,*N*-diethyl formamide (DEF)/methanol/H_2O (2∶1∶2, *V*/*V*). Then the solution was sealed in a 23 mL Teflon-lined stainless steel autoclave and heated under autogenous pressure at 100 ℃ for three days. The colorless crystals were collected, washed with ethanol and dried in the air. Yield: 40% (based on (R)-H_3CIA). Anal. Calcd. for $C_{47}H_{34}Cd_3N_5O_{16}$(%): C, 44.73; H, 2.72; N, 5.58. Found(%): C, 42.24; H, 2.42; N, 5.04. IR (KBr, cm^{-1}): 3 403(m), 1 603(s), 1 559(s), 1 417(m), 1 367(m), 1 448(m), 1 250(w), 1 219(w), 804(w), 631(w).

1.3 Synthesis of $[Zn_3((R)\text{-}CIA)(bmib)_2(H_2O)_2Cl]\cdot H_2O\cdot x$Guest (2)

A mixture of $ZnCl_2$ (27 mg, 0.2 mmol), bmib (48 mg, 0.2 mmol), (*R*)-H_3CIA (25 mg, 0.1 mmol) and pyrazine (80 mg, 1 mmol) was dissolved in 4 mL *N*,*N*-dimethyl acetamide (DMA)/H_2O (1∶1, *V*/*V*). Then the solution was sealed in a 23 mL Teflon-lined stainless steel autoclave and heated under autogenous pressure at 120 ℃ for three days. The colorless crystals were collected, washed with ethanol and dried in the air. Yield: 30% (based on (*R*)-H_3CIA). Anal. Calcd. for $C_{39}H_{36}ClN_8O_{7.50}Zn_2$ (%): C, 51.88; H, 4.02; N, 12.41. Found(%): C, 48.72; H, 3.64; N, 10.96. IR (KBr, cm^{-1}): 3 453(m), 3 137(w), 1 621(m), 1 584(m), 1 516(s), 1 411(s), 1 300(m), 1 151(m), 1 108(m), 1 008(m), 841(m), 737(m), 669(m), 563(w), 507(w).

1.4 Crystal structural determination

The data of **1** and **2** were collected on a Rigaku four-circle 003 CCD diffractometer using graphite monochromated Mo $K\alpha$ radiation (λ=0.071 073 nm) at room temperature. The integration and reduction of

data were performed with Rigaku OD 2015 software. Empirical absorption corrections were applied by using spherical harmonics, implemented in SCALE3 ABSPACK scaling algorithm. The structures of complexes were solved by the direct methods in Olex2-1.2 using SHELXS-2017 and refined on F^2 by full-matrix least-squares using the SHELXL-2017 program package[14-15]. All the hydrogen atoms were placed on their calculated positions and treated as riding atoms with default parameters. Some disordered guest molecules in frameworks could not be identified by X-ray single crystal structure analysis. Furthermore, because complexes **1** and **2** were synthesized in mixed solvents, the disordered guest molecules also could not be decided by TGA and elemental analysis. For these reasons, the disordered guest molecules had to be subtracted from the reflection data through the SQUEEZE method and further discussions were not performed[16]. Crystallographic data and experimental details for structural analysis are summarized in Table 1, and selected bond lengths and angles of complexes **1~2** are summarized in Table 2.

CCDC: 1920451, **1**; 1920452, **2**.

Table 1　Crystal data and structure refinement details for complexes 1 and 2

Complex	**1**	**2**
Formula	$C_{47}H_{34}Cd_3N_5O_{16}$	$C_{39}H_{36}ClN_8O_{7.50}Zn_2$
Formula weight	1 261.99	902.95
Crystal system	Monoclinic	Orthorhombic
Space group	$P2$	$P2_12_12$
a / nm	1.030 42(4)	3.437 13(14)
b / nm	1.173 80(4)	1.598 41(7)
c / nm	2.411 63(11)	0.756 69(3)
β / (°)	98.101(4)	
V / nm^3	2.887 8(2)	4.157 2(3)
Z	2	2
D_c / (g·cm^{-3})	1.451	1.443
Absorption coefficient / mm^{-1}	1.158	1.277
F(000)	1 246	1 852
θ range / (°)	4.035 0~30.309 0	3.918 0~30.523 0
GOF	1.000	0.973
R_1[a] [$I>2\sigma(I)$]	0.028 9	0.042 5
wR_2[b] (F^2) [$I>2\sigma(I)$]	0.067 0	0.091 4
Final R_1 value (all data)	0.032 9	0.067 6
Final wR (F^2) value (all data)	0.068 1	0.097 3
Flack parameter	0.006(11)	−0.006(5)

[a] $R_1=\sum||F_o|-|F_c||/\sum|F_o|$; [b] $wR_2=[\sum w(F_o^2-F_c^2)^2/\sum w(F_o^2)^2]^{1/2}$.

Table 2　Selected bond length (nm) and angles (°) for 1 and 2

1					
Cd(1)-O(5)#1	0.232 0(3)	Cd(1)-N(2)#2	0.229 0(4)	Cd(2)-O(2)	0.244 1(4)
Cd(1)-O(4)	0.232 1(3)	Cd(1)-O(7)#3	0.244 4(3)	Cd(2)-O(2W)	0.230 2(4)
Cd(1)-N(1)	0.232 9(4)	Cd(1)-O(3)#3	0.240 0(3)	Cd(2)-O(1)	0.245 1(4)
Cd(2)-N(3)	0.236 1(4)	Cd(2)-O(8)	0.234 8(5)	Cd(2)-O(9)	0.247 7(5)
Cd(2)-O(1W)	0.231 3(6)	Cd(3)-O(12)#4	0.229 7(3)	Cd(3)-O(13)#3	0.242 0(3)
Cd(3)-O(11)	0.226 6(3)	Cd(3)-O(14)#3	0.240 3(3)	Cd(3)-N(4)	0.234 3(4)
Cd(3)-N(5)#2	0.231 5(4)				

Continued Table 2

O(5)#1-Cd(1)-O(7)#2	136.95(10)	O(4)-Cd(1)-O(6)#2	85.39(10)	N(1)-Cd(1)-O(7)#2	99.51(14)
N(1)-Cd(1)-O6#2	86.34(14)	N(2)#3-Cd(1)-O(5)#1	87.67(13)	N(2)-Cd(1)-O(4)	89.63(13)
N(2)-Cd-N(1)	173.45(12)	N(2)#3-Cd(1)-O(7)#2	85.26(12)	N(2)#3-Cd(1)-O(6)	100.13(13)
O(6)#2-Cd(1)-O(7)#2	53.84(10)	O(12)#4-Cd(3)-O(13)#2	93.42(11)	O(12)#4-Cd(3)-O(14)#2	147.13(11)
O(12)#4-Cd(3)-N(4)	87.98(13)	O(12)#4-Cd(3)-N(5)#3	88.38(14)	O(11)-Cd(3)-O(12)#4	126.88(11)
O(11)-Cd(3)-O(13)#2	139.65(10)	O(11)-Cd(3)-O(14)#2	85.71(10)	O(11)-Cd(3)-N(4)	91.11(14)
O(11)-Cd(3)-N(5)#3	89.56(15)	O(14)#2-Cd(3)-O(13)#2	54.37(10)	N(4)-Cd(3)-O(13)#2	88.21(14)
N(4)-Cd(3)-O(14)#2	96.43(13)	N(5)#3-Cd(3)-O(13)#2	93.90(14)	N(5)#3-Cd(3)-O(14)#2	87.66(13)
N(5)#3-Cd(3)-N(4)	175.89(12)	O(2)-Cd(2)-O(1)	53.91(12)	O(2)-Cd(2)-O(9)	167.94(13)
O(2W)-Cd(2)-O(2)	82.15(14)	O(2W)-Cd(2)-O(1)	86.42(15)	O(2W)-Cd(2)-N(3)	167.76(14)
O(2W)-Cd(2)-O(8)	94.41(16)	O(2W)-Cd(2)-O(9)	91.04(15)	O(2W)-Cd(2)-O(1W)	88.6(2)
O(1)-Cd(2)-O(9)	135.91(14)	N(3)-Cd(2)-O(2)	85.67(13)	N(3)-Cd(2)-O(1)	85.46(14)
N(3)-Cd(2)-O(9)	101.16(15)	O(8)-Cd(2)-O(2)	136.43(13)	O(8)-Cd(2)-O(1)	82.57(14)
O(8)-Cd(2)-N(3)	93.60(15)	O(8)-Cd(2)-O(9)	53.72(14)	O(1W)-Cd(2)-O(2)	80.8(2)
O(1W)-Cd(2)-O(1)	134.7(2	O(1W)-Cd(2)-N(3)	90.7(2)	O(1W)-Cd(2)-O(8)	142.7(2)
O(1W)-Cd(2)-O(9)	89.1(2)	O(5)#1-Cd(1)-O(4)	129.37(10)	O(5)#1-Cd(1)-N(1)	87.59(14)
		2			
Zn(2)-O(1)#1	0.196 8(3)	Zn(2)-O(1)	0.196 8(3)	Zn(2)-N(8)#2	0.202 1(3)
Zn(2)-N(8)#3	0.202 1(3)	Zn(1)-O(6)	0.194 4(3)	Zn(1)-O(4)#4	0.193 6(3)
Zn(1)-N(1)	0.204 1(3)	Zn(1)-N(5)	0.200 4(3)	Zn(3)-Cl(1)	0.222 91(14)
Zn(3)-Cl(1)#5	0.222 91(14)	Zn(3)-N(4)	0.203 5(3)	Zn(3)-N(4)#5	0.203 5(3)
O(1)#1-Zn(2)-O(1)	94.36(17)	O(1)-Zn(2)-N(8)#2	103.08(12)	O(1)#1-Zn(2)-O(8)#3	103.09(12)
O(1)#1-Zn(2)-O(8)#2	127.43(13)	O(1)-Zn(2)-N(8)#3	127.43(13)	N(8)#3-Zn(2)-N(8)#2	104.3(2)
O(6)-Zn(1)-N(1)	98.59(14)	O(6)-Zn(1)-N(5)	132.51(13)	O(6)-Zn(1)-N5	132.51(13)
O(4)#4-Zn(1)-O(6)	107.78(15)	O(4)#4-Zn(1)-N(1)	99.98(13)	O(4)#4-Zn(1)-N(5)	109.39(14)
N(5)-Zn(1)-N(1)	102.94(15)	Cl(1)-Zn(3)-Cl(1)#3	115.70(9)	N(4)#5-Zn(3)-Cl(1)	107.46(11)
N(4)-Zn(3)-Cl(1)#5	107.46(11)	N(4)#5-Zn(3)-Cl(1)#5	109.24(12)	N(4)-Zn(3)-Cl(1)	109.23(12)
N(4)#5-Zn(3)-N(4)	107.5(2)				

Symmetry codes: #1: $-x$, y, $1-z$; #2: x, $1+y$, z; #3: $-1+x$, y, z; #4: $-x$, y, $-z$ for **1**; #1: $2-x$, $1-y$, z; #2: $2-x$, $1-y$, $2+z$; #3: x, y, $2+z$; #4: $3/2-x$, $1/2+y$, $2-z$; #5: $1-x$, $1-y$, z for **2**.

2 Results and discussion

2.1 Crystal structure of $[Cd_3((R)\text{-}CIA)_2(bipy)_{2.5}(H_2O)_2]\cdot x$Guest (1)

X-ray single crystal structure analysis reveals that complex **1** crystallizes in monoclinic chiral space group $P2$ with Flack parameter of 0.006(11). The asymmetric unit of **1** is comprised of three Cd^{2+} centers, two deprotonated (*R*)-CIA^{3-} ligands, two and a half bipy ligands and two coordinated water molecules. Each of (*R*)-CIA^{3-} ligand as κ_6-linker is connected by four Cd^{2+} centers. For the unique coordination modes of (*R*)-CIA^{3-} ligands, two dinuclear clusters $Cd_2(CO_2)_4$ are formed (Fig.1). In the $Cd_2(CO_2)_4$ clusters, Cd1 and Cd3 centers with similar octahedral geometries are coordinated by four oxygen atoms from three carboxylate groups of three isophthalic units and two nitrogen atoms from two bipy ligands, respectively. Unlike Cd1 and Cd3, Cd2 adopts pentagonal dipyramidal configuration, and is coordinated by a nitrogen atom of bipy ligand, four carboxylate oxygen atoms from two lactate units and two water molecules.

Because the framework of **1** contains two distinct ligands (bipy and (*R*)-CIA^{3-}), to further simplify the complicated 3D frameworks, we divide the whole framework into two part according to the different

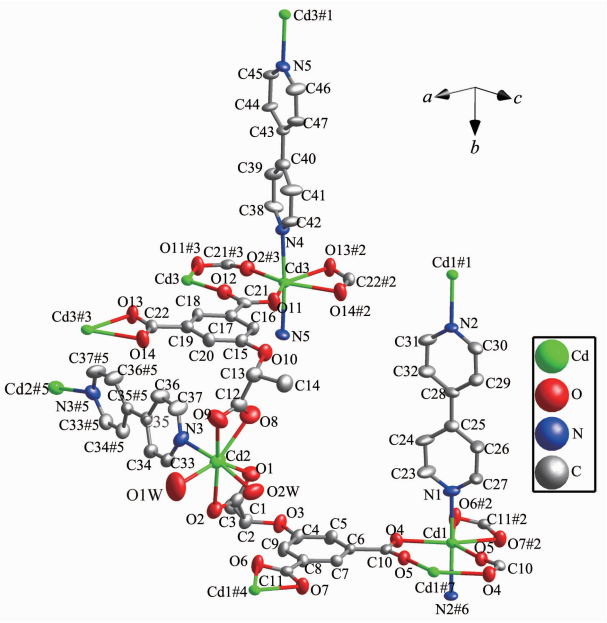

Ellipsoid probability level: 50%; Symmetry codes: #1: x, $-1+y$, $-z$; #2: $-1+x$, y, z; #3: $-x$, y, $-z$; #4: $1+x$, y, z; #5: $1-x$, y, $-z$; #6: x, $1+y$, z; #7: $-x$, y, $1-z$

Fig.1　Coordination environment of Cd(Ⅱ) ions in complex **1**

ligands. If the connectivity between Cd(Ⅱ) ions and (*R*)-CIA^{3-} are only considered, a 2D Cd-(*R*)-CIA layer is generated (Fig.2). In the Cd-(*R*)-CIA layer, the dinuclear $Cd_2(CO_2)_4$ is 4-connected node and the (*R*)-CIA^{3-} is 3-connected node. Thus, the 2D Cd-(*R*)-CIA layer of **1** can be described as a (3, 4)-connected net (Fig.2b). The adjacent Cd-(*R*)-CIA layers are further linked together by bipy ligands to form a 3D pillared-layer framework (Fig.2c). In the 3D framework, (*R*)-CIA^{3-} ligands still act as 3-connected nodes. Each $Cd_2(CO_2)_4$ cluster as 6-connected node are linked by four (*R*)-CIA^{3-} ligands and four bipy ligands, and each Cd3 ion is linked by two (*R*)-CIA^{3-} ligands and a bipy ligand as 3-connected nodes. As a result, the whole 3D framework of **1** is topologically represented as a (3,3,3,6,6)-connected net with a point symbol of $(4.5^2)_2(4.8^2)2(4^2.6^8.8^3.10^2)(4^2.6^8.8^3.9^2)(5.8.9)_2$[17].

2.2　Crystal structure of $[Zn_3((R)\text{-CIA})(bmib)_2(H_2O)_2Cl]\cdot H_2O\cdot x$Guest (2)

Complex **2** crystallizes in orthorhombic space

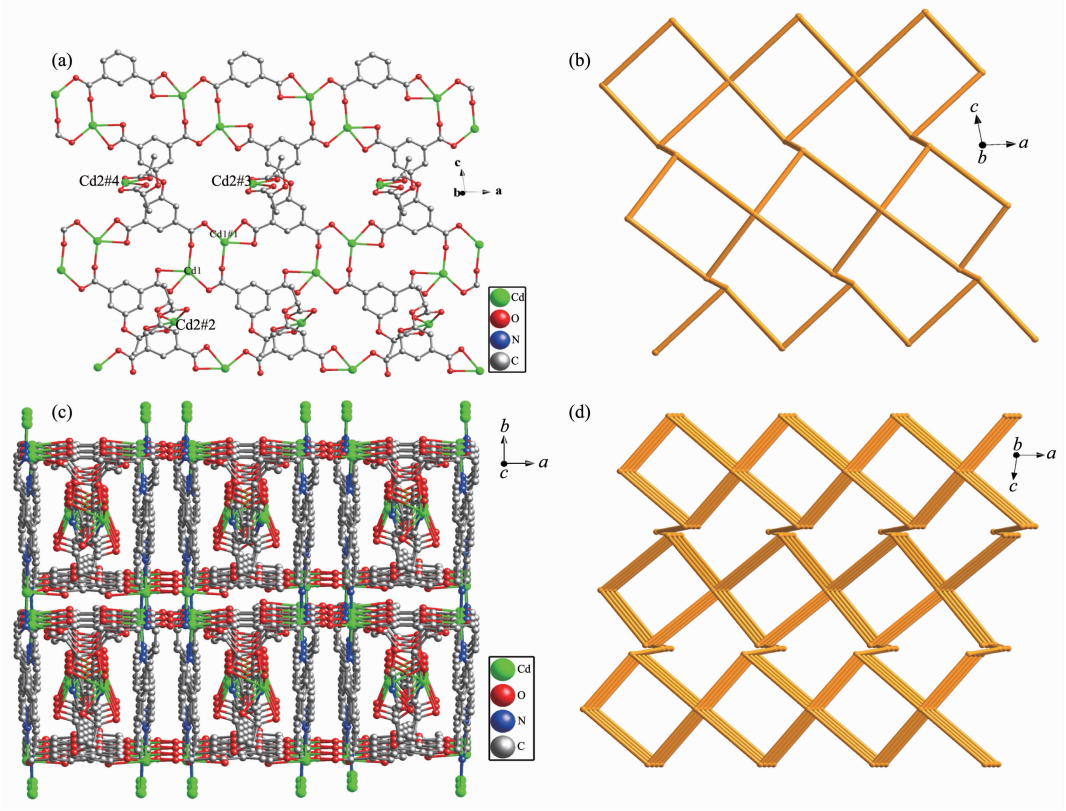

Symmetry codes: #1: $-x$, y, $1-z$; #2: $-1+x$, y, z; #3: $1-x$, y, $1-z$; #4: $-x$, y, $1-z$

Fig.2　Schematic illustration of **1**: (a) 2D Cd-(*R*)-CIA layer; (b) topological net of Cd-(*R*)-CIA layer; (c) 3D framework constructed by Cd-(*R*)-CIA layers and bipy ligands; (d) 3,3,3,6,6-connected 3D net

group $P2_12_12$ with Flack parameter of −0.006(5). As shown in Fig.3, there are two Zn(Ⅱ) ions, one (*R*)-CIA^{3-} ligand, one chloride ion, two bmib ligands and a guest water molecules in a asymmetric unit of complex **2**. Zn1 is in tetrahedral coordination surrounded by two O atoms from two lactate units of (*R*)-CIA^{3-} and two N atoms from bmib ligands. Zn2 is similar to Zn1 and is coordinated by two O atoms from two isophthalic acid units of (*R*)-CIA^{3-} and two N atoms from two bmib ligands, forming a tetrahedral coordination environment. Zn3 also adopts a tetrahedral geometry as Zn1 and Zn2, coordinated by two chloride ions and two N atoms from two bmib ligands.

In complex **2**, if only the connectivity between isophthalic acid units of (*R*)-CIA^{3-} and Zn1 ions is considered, a right-handed helical chain is generated along *b*-axis (Fig.4a). And then a helical 2D (*R*)-CIA-Zn layer is formed by the right-handed helical chains,

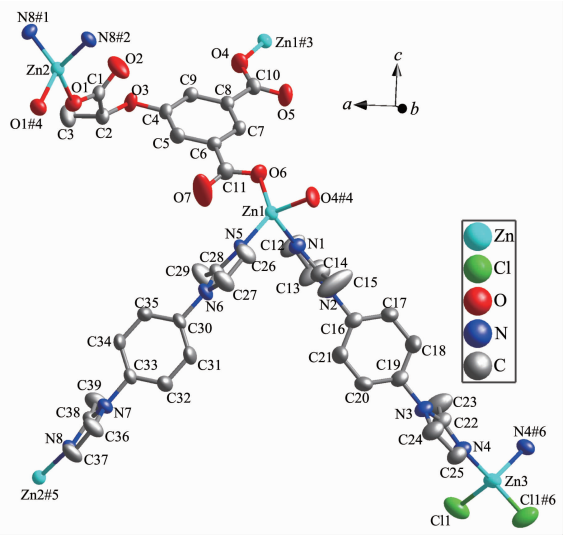

Ellipsoid probability level: 50%; Symmetry codes: #1: 2−*x*, 1−*y*, 2+*z*; #2: *x*, *y*, 2+*z*; #3: 1.5−*x*, −0.5+*y*, 2−*z*; #4: 1.5−*x*, 0.5+*y*, 2−*z*; #5: *x*, *y*, −2+*z*; #6: 1−*x*, 1−*y*, *z*

Fig.3 Coordination environment of Zn(Ⅱ) ions in complex **2**

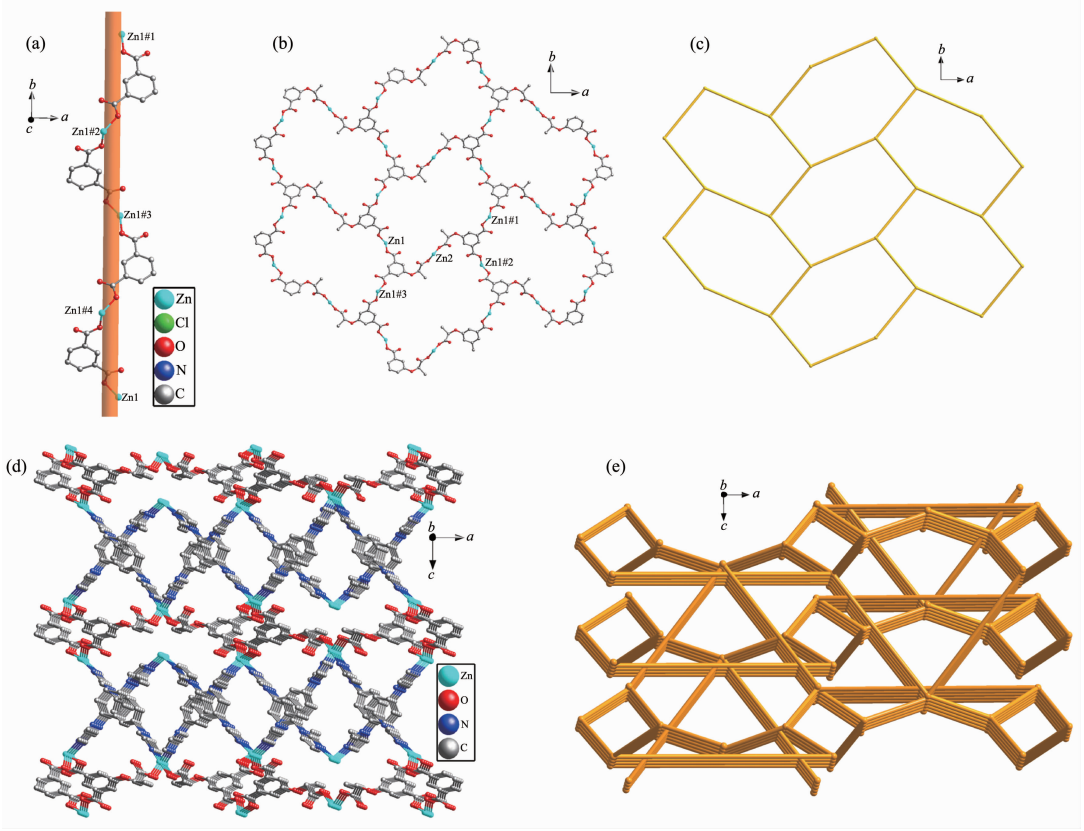

Symmetry codes: #1: *x*, 2+*y*, *z*; #2:1.5−*x*, 1.5+*y*, 2−*z*; #3: *x*, 1+*y*, *z*; #4: 1.5−*x*, 0.5+*y*, 2−*z* in (a); #1: 0.5+*x*, 1.5−*y*, 2−*z*; #2: 2−*x*, 1−*y*, 2−*z*; #3: 1.5−*x*, −0.5+*y*, 2−*z* in (b)

Fig.4 Schematic illustration of **2**: (a) right-handed helical chain constructed by (*R*)-CIA^{3-} fragments and Zn(Ⅱ) ions; (b) 2D (*R*)-CIA-Zn layer; (c) *hcb* net of Zn-(*R*)-CIA layer; (d) 3D framework constructed by Zn-(*R*)-CIA layers and bmib ligands; (e) (3,4,4)-connected topological net

lactate units and Zn(3) ions (Fig.4b). In the (*R*)-CIA-Zn layer, the (*R*)-CIA^{3-} ligands can be viewed as 3-connected nodes, thus it can be reduced into a *hcb* net (Fig.4c) [17]. Finally, the adjacent (*R*)-CIA-Zn layers are further linked together by bmib ligands, resulting in a 3D nonclassical pillared-layer framework (Fig.4d). In the 3D framework, the (*R*)-CIA^{3-} ligands act as three-connected nodes, Zn1 and Zn2 centers are regarded as 4-connected nodes, respectively, and bmib ligands are only simple linkers. Therefore, the whole framework of **2** is topologically represented as a 3,4,4-connected net with a point symbol of $(6\cdot7^2)_2(6\cdot7^5)_2(6^2\cdot7^4)$ (Fig.4d)[17].

2.3 Structural diversities of complexes 1 and 2

As far as complexes **1** and **2** are concerned, the same enantiomeric ligands but different metal ions and auxiliary ligands are used to construct the corresponding frameworks. From the structural descriptions above, chiral ligand plays different roles in the construction of various structures. In complex **1**, the (*R*)-CIA^{3-} ligands as κ_6-linkers present two similar conformations to connect four Cd (Ⅱ) centers to construct a 2D (*R*)-CIA-Cd layer. In the (*R*)-CIA-Cd layer, two dinuclear clusters $Cd_2(CO_2)_4$ are formed by rigid isophthalic acid units of (*R*)-CIA^{3-} ligands and Cd (Ⅱ) centers. Compared with complex **1**, rigid isophthalic acid units of (*R*)-CIA^{3-} ligands and Zn(Ⅱ) centers build an interesting right-handed helical chain in complex **2**. The right-handed helical chain are further linked together to give rise to a 2D (*R*)-CIA-Zn layer by lactate units of (*R*)-CIA^{3-} ligands and Zn ions. Apparently, the different metal ions lead to the (*R*)-CIA^{3-} ligands with different coordination modes in complex **1** and **2**. Besides the effects of metal ions, the significant structural differences of the complexes should be also ascribed to the introduction of the auxiliary N-donor ligands, which makes complexes **1** and **2** show 3D pillar-layered framework.

2.4 Circular dichroism

To further study their chiral characteristic, bulk crystal samples of complexes **1** and **2** were selected to measure the solid-state circular dichroism (CD) spectra in KCl plates between 200 and 600 nm. As shown in Fig.5, there is an obvious Cotton effect at 268 nm in the spectra of complex **1**. Furthermore, complex **2** had two positive CD signals at 255 and 285 nm, and a negative CD signal at 275 nm. These results confirm that the bulk samples of complexes **1** and **2** are homochiral, and chirality of ligand (*R*)-H_3CIA can be transferred to the corresponding coordination complex aggregates.

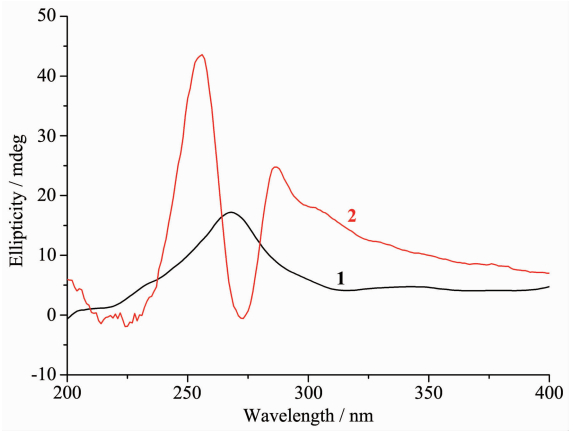

Fig.5 Solid-state CD spectra of complexes **1** and **2**

2.5 Photoluminescence properties

Fluorescence properties of the inorganic-organic hybrid coordination polymers containing d^{10} metal have attracted considerable attention for their potential applications. Hence, the solid-state photoluminescent spectra of complexes **1** and **2** were investigated at room temperature. As depicted in Fig.6, the photoluminescence spectra have emission peaks with maxima at 464 nm (λ_{ex}=358 nm) for **1**, and 441 nm (λ_{ex}=348 nm) for **2**. To better understand the nature of

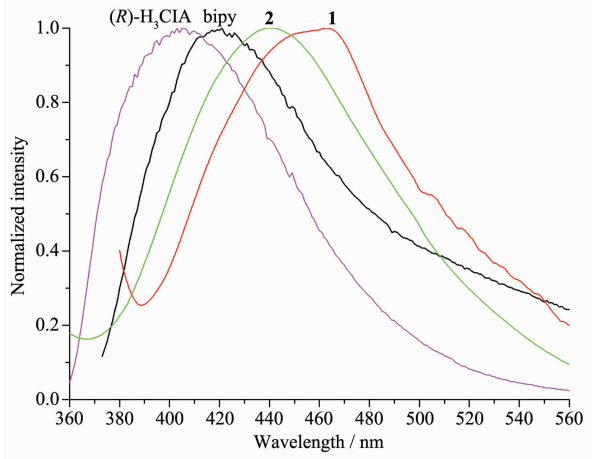

Fig.6 Photoluminescence spectra of the ligands and complexes

the emission band, the photoluminescence spectra of ligands (*R*)-H_3CIA and bipy were also measured. The results showed that (*R*)-H_3CIA displayed an emission band at 404 nm (λ_{ex}=336 nm), while bipy ligand had emission peak with maxima at 420 nm (λ_{ex}=353 nm). As compared to the ligands, emission maxima of **1** and **2** have distinct red-shifts, respectively, which should be ascribed to intraligand (n-π* or π-π*) emission[18-19].

3 Conclusions

In summary, two homochiral coordination polymers (HCPs) have been synthesized by using lactic acid derivative (*R*)-H_3CIA as chiral ligand with the help of rigid auxiliary ligands. In HCPs **1** and **2**, the (*R*)-CIA^{3-} ligands can adopt different binding sites with metal ions to build various pillar-layered frameworks. The successful synthesis of complexes **1** and **2** shows that (*R*)-H_3CIA is a class of effective chiral ligand for constructing HCPs due to its inherent chirality and multiple coordination modes.

Supporting information is available at http://www.wjhxxb.cn

References:

[1] Agranat I, Caner H, Caldwell J. *Nat. Rev. Drug Discovery*, **2002**,**1**:753-768

[2] Barron L D. *Nature*, **2000**,**405**:895-896

[3] Tan C X, Han X, Li Z J, et al. *J. Am. Chem. Soc.*, **2018**,**140**: 16229-16236

[4] Yoon M, Srirambalaji R, Kim K. *Chem. Rev.*, **2012**,**112**: 1196-1231

[5] Han Q, He C, Zhao M, et al. *J. Am. Chem. Soc.*, **2013**,**135**: 10186-10189

[6] Mihalcea I, Zill N, Mereacre V, et al. *Cryst. Growth Des.*, **2014**,**14**:4729-4734

[7] Wen Y H, Sheng T L, Sun Z H, et al. *Chem. Commun.*, **2014**,**50**:8320-8323

[8] Kumar N, Khullar S, Singh Y, et al. *CrystEngComm*, **2014**, **16**:6730-6744

[9] Dubey M, Kumar A, Dhavale V A, et al. *CrystEngComm*, **2015**,**17**:8202-8206

[10]JI Qin(吉沁), CHENG Li-Zhuang(陈立庄). *Chinese J. Inorg. Chem.*(无机化学学报), **2017**,**33**(5):874-880

[11]Xu Z X, Xiao Y, Kang Y, et al. *Cryst. Growth Des.*, **2015**, **15**:4676-4686

[12]Xu Z X, Liu L Y, Zhang J. *Inorg. Chem.*, **2016**,**55**:6355-6357

[13]Gu Z G, Zhang C H, Zhang J, et al. *Chem. Soc. Rev.*, **2016**, **45**:3122-3144

[14]Dolomanov O V, Bourhis L J, Gildea R J, et al. *J. Appl. Cryst.*, **2009**,**42**:339-341

[15]Sheldrick G M. *Acta Crystallogr. Sect. C*: *Cryst. Struct. Commun.*, **2015**,**C71**:3-8

[16]Speck A L. *Acta Crystallogr. Sect. C*: *Cryst. Struct. Commun.*, **2015**,**C71**:9-18

[17]Aexandrov E V, Blatov V A, Kochetkov A V, et al. *CrystEngComm*, **2011**,**13**:3947-3958

[18]LIU Lu(刘露), LI Ying(李英), WANG Jian-Ji (王键吉), et al. *Chinese J. Inorg. Chem.*(无机化学学报), **2019**,**35**(3): 546-552

[19]Cui P, Chen Z, Gao D L, et al. *Cryst. Growth Des.*, **2010**,**10**: 4370-4378